



SANDWICH STRUCTURES WITH FOLDED CORE: MANUFACTURING AND MECHANICAL BEHAVIOR

SEBASTIAN FISCHER

Universität Stuttgart, Institut für Flugzeugbau, 70569 Stuttgart, Germany

SEBASTIAN HEIMBS

EADS Innovation Works, 81663 Munich, Germany

SEBASTIAN KILCHERT

German Aerospace Center (DLR), 70569 Stuttgart, Germany

MICHAEL KLAUS

RWTH Aachen University, Department of Aerospace and Lightweight Structures,
52062 Aachen, Germany

CHRISTOPH CLUZEL

LMT Cachan, 94235 Cachan Cedex, France

SUMMARY

A foldcore is an origami-like structural sandwich core, which is manufactured by folding a planar base material into a three-dimensional structure. The development of foldcores and production methods is carried out at the moment at the University of Stuttgart in Germany and the Kazan State Technical University in Russia. Within the project CELPACT various foldcores with different unit cell geometries and different base materials were produced and tested, including flatwise compression tests and transverse shear tests. Also the base materials were tested in tension and compression tests in order to obtain their material data.

1. INTRODUCTION

The main manufacturing step is folding the base material into a three-dimensional structure (Fig. 1a). The folding technique allows different types of unit cell geometries. In the work for CELPACT, two types of unit cells are used. These are the “zigzag” or “2-HAP” (two pairs of principal axes, the material is folded around two axes) unit cell geometry (Fig. 1b) and the “3-HAP” unit cell geometry (Fig. 1c). The main application for foldcores is the usage as structural sandwich cores, for which they are predestined by featuring high strength and stiffness to weight ratios. Furthermore, their mechanical properties can be adjusted to the application by varying the unit cell geometry and the base material. Beyond their mechanical properties, foldcores feature also multifunctional aspects. Good thermal insulation and acoustic damping are two characteristics which they share with other sandwich core materials like honeycombs. An advantage to honeycomb cores is the open cellular design, which allows ventilation through the open foldcore channels (Fig. 1d).

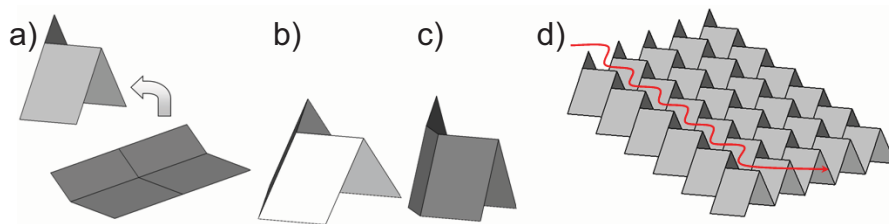


Figure 1:
Principle of folding the flat base material into the three-dimensional foldcore (a), the zigzag and the 3-HAP unit cell (b+c) and the ventilation of foldcores through open channels (d).

2. KAZAN-TYPE FOLDCORE

The discontinuously produced folded cores in this study were manufactured at the Kazan State Technical University in Russia. The manufacturing process is based on the forming of a flat sheet of cell wall material between two matrices [1,2]. But in contrast to deep drawing, the matrices are transformable so that the prepreg material is folded without being elongated. In this study the folded cores were made from prepreg sheets of carbon fiber/epoxy (CFRP) in a $[0^\circ/90^\circ/0^\circ]$ lay-up of unidirectional (UD) plies (Fig. 2a) or woven fabric plies (Fig. 2b). Different zigzag geometries were analyzed in this study.

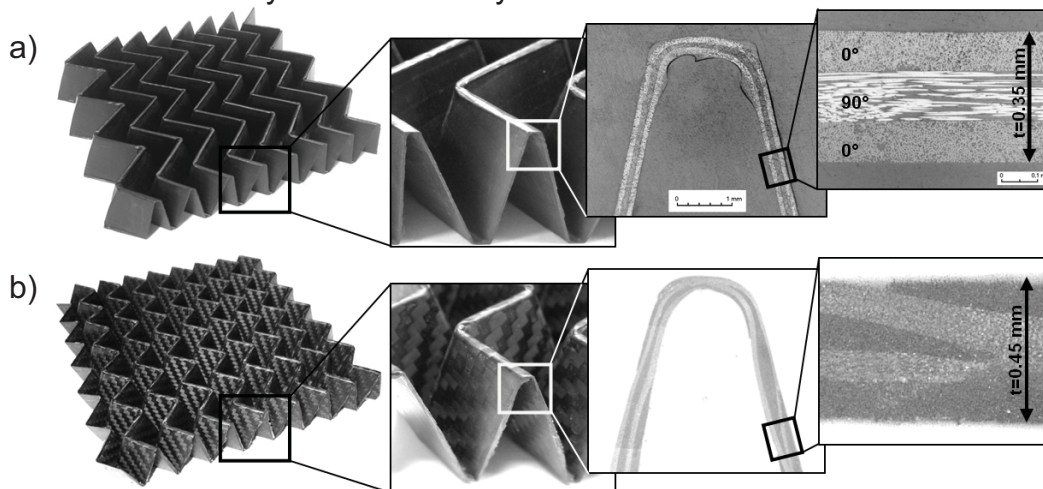


Figure 2:
Discontinuously produced folded core structures made of CFRP. Unidirectional cell wall material, large cell walls (a), woven fabric cell wall material, small cell walls (b).

3. STUTTGART-TYPE FOLDCORE

For CELPACT, foldcore samples with different unit cell geometries and base materials were produced at the University of Stuttgart where discontinuous and continuous production methods are currently in use and in further development [3]. Samples for static testing were produced from preimpregnated aramid paper and from aluminum foil. Foldcores from aramid paper with four different 3-HAP unit cell geometries were produced and investigated (Fig. 3a-d). Also aluminum foldcores with a 2-HAP unit cell were manufactured and used for different tests (Fig. 3e) [4]. Fig. 3f shows a real-life specimen of a foldcore type 31.

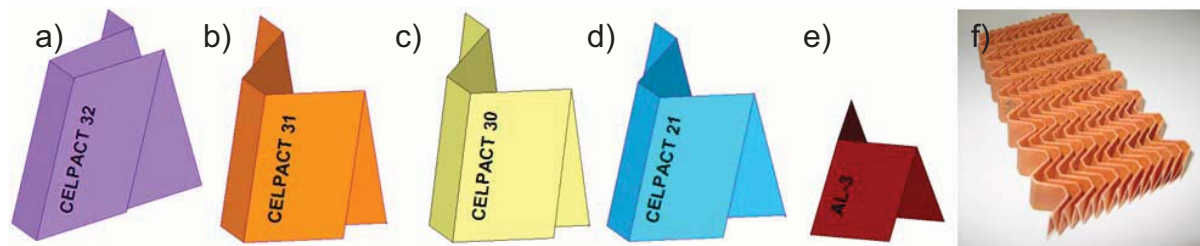


Figure 3: Unit cells of the in CELPACT investigated aramid paper and aluminum foldcores: blocked 3-HAP unit cell type 32 (a), 3-HAP unit cells type 31, 30 and 21 (b,c,d). And 2-HAP unit cell of aluminum foldcore type AL-3 (e). Sample of foldcore type 31 (f).

4. TEST PROGRAM ON BASE MATERIALS

4.1 Test program on base material for Kazan-type foldcores

The mechanical properties of the CFRP cell wall material of the discontinuously produced folded cores were determined in 0° tensile tests and $\pm 45^\circ$ tensile tests (in-plane shear properties). Compression test data were provided by the CFRP material manufacturer Krempel. In contrast to the rather ductile aramid paper cell walls, the CFRP shows a very brittle behavior with low breaking elongations and significantly higher stiffness and strength properties.

4.2 Test program on base material for Stuttgart-type foldcores

4.2.1 Microscale observations of aramid paper

Aramid fibers are not uniformly distributed over the paper thickness. An analysis with an optical microscope on a polished cut section (Fig. 4a) shows that the paper can be considered as a three-layer laminate. The internal layer is composed of aramid fibers randomly distributed and phenolic matrix whereas the two external layers are poor in fibers and mainly made of phenolic resin with a rough aspect. Fibers are randomly oriented in the in-plane directions but some of them agglomerate in small bundles (Fig. 4b), which may affect the damage evolution under tensile loading.

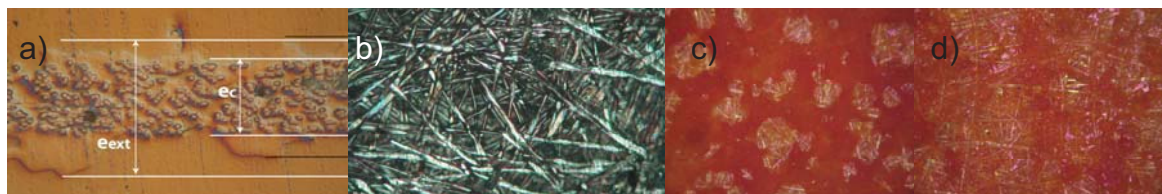


Figure 4: Paper thickness micrograph (a) and distribution of fibers through the paper (b). Aspect of paper face A (top side) (c) and aspect of paper face B (lower side) (d).

The fiber-matrix distribution has an effect on the elastic properties. Traction and bending tests have been performed. For the tensile test, strain was determined both by an extensometer and digital image correlation technique. The bending test is a free vibration test with laser-velocimeter measurement. The first eigenfrequency value makes it possible to determine the average bending

stiffness. By knowing the phenolic matrix Young's modulus ($E_m = 3 \text{ GPa}$) and by measuring the internal layer thickness ($e_c = 0.2 \text{ mm}$), it is then possible to determine the total paper thickness ($e_{\text{ext}} = 0.33 \text{ mm}$) as well as the Young's modulus of the internal layer ($E_c = 5.57 \text{ GPa}$). Buckling tests on a plane paper sample were also performed. It was shown that 90% of the samples bent in a particular direction such that the face B (Fig. 4d) of the sample was under tension whereas face A (Fig. 4c) is under compression. It is consequently recommended to differentiate the elastic properties of the two external layers for the laminate model used in simulation.

The first crack on face B was observed by a Scanning Electron Microscope (Fig. 5a). It behaves like a plastic hinge for higher bending level (Fig. 5b). Fiber debonding occurs without total rupture. Fibers still bridge the two crack faces up to the complete paper fold.

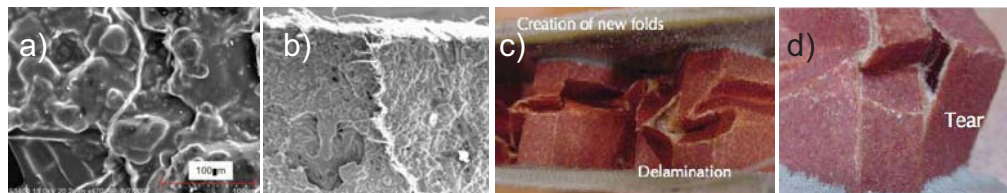


Figure 5: First crack in the face B external layer (a), plastic hinge formation at high bending level (b), creation of new folds and delamination (c) and tear along an initial fold (d).

4.2.2 Mesoscale observations of aramid paper

Analysis of the core during flatwise compression test exhibits three meso-degradation mechanisms. Fig. 5c shows the creation of folds that corresponds to plastic hinges as described previously. A delamination mechanism also occurs from the initial folds (Fig. 5c). The paper split through the thickness into two sheets, which both fold. The last mechanism is the tear of an initial fold (Fig. 5d). The buckling tests also allow evaluating the nonlinear behavior of a paper sample (Fig. 6a). A comparison between the elastic simulation and experimental results (Fig. 6b) shows that material nonlinearities occur prior to the critical buckling load. A nonlinear material model has to be introduced to predict the peak stress for the fold core compressive test.

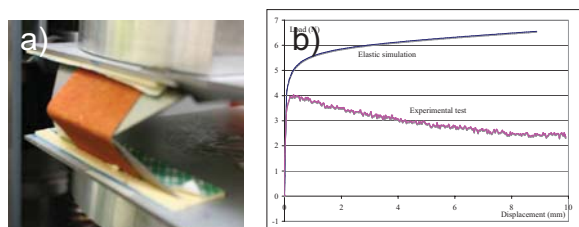


Figure 6: Buckling test on a paper sample (a) and Load-displacement curve (b)

4.2.3 Cylinder compression tests

To investigate the aramid paper compressive behavior a test series of small thick-walled cylinder was conducted. Fig. 7a depicts the cylinder dimensions and Fig. 7b shows a compressed sample in the testing machine. The initial elastic behavior of the cylinder as seen in Fig. 7c corresponds to other compressive tests performed within the CELPACT project [5]. Fig. 7b depicts the compression test sample for a large compression strain where the circular kink is distinctly

visible. Delaminations are forming sharp kink folds at the inside and outside of the cylinder wall but the crushing behavior seems to be dominant.

It is noted that the plateau compression stresses after the stress drop are considered to give basic information about the aramid paper compression and plastic yield properties needed in the material model. It was concluded that the nonlinear compressive behavior is mainly matrix driven and features almost perfect plastic properties.

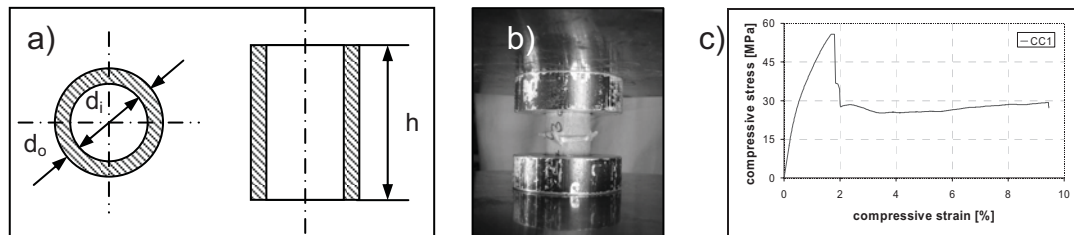


Figure 7:

Dimensions of thick-walled cylinder (a), image of a specimen forming a circular kink (b) and stress-strain curve of thick-walled cylinder sample (c).

5. TEST PROGRAM ON FOLDCORE SANDWICH STRUCTURES

5.1 Test program on Kazan-type foldcores

The CFRP foldcores were tested in flatwise compression and transverse shear (Fig. 8) on an Instron universal testing machine [6]. For this purpose, composite skins have been bonded onto the core with the epoxy-based adhesive Epibond 1590 A/B to produce sandwich specimens of 150 mm x 150 mm.

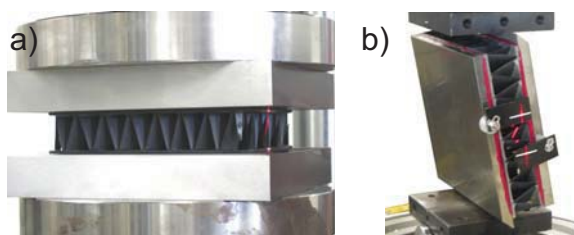


Figure 8:

Compression (a) and transverse shear test (b) of CFRP folded core

5.2 Test program on Stuttgart-type foldcores

A test program was performed to acquire the basic mechanical properties of foldcores. The test program was focused on panels with 3-HAP foldcores with cell walls made of aramid paper. Cores with different types of folding geometry were tested. Two test set-ups were used for the test program to perform shear (standards DIN 53294 and ASTM C273) and flatwise compression tests (standards DIN 53291 and ASTM C 365-00) [7]. Due to the design of the foldcores, the transverse shear tests were performed in two principal directions of the core.

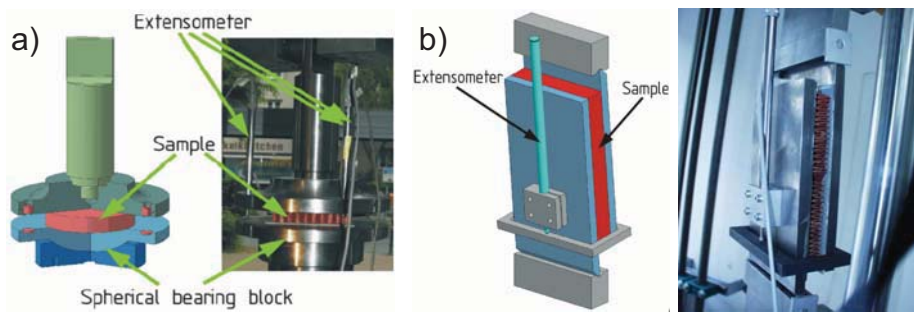


Figure 9:
 Setup for flatwise compression test (a) and for transverse shear test (b).

6. RESULTS FROM TESTS ON FOLDCORE SANDWICH STRUCTURES

6.1 Test results for Kazan-type foldcores

The flatwise compressive behavior of the CFRP foldcore is dominated by a cell wall fracture after initial buckling. The angular geometry leads to a loss of contact and load transfer between the upper and lower side resulting in a drop of the stress level to low values. As the compression continues, more cell walls come into contact and are crushed at the opposite side leading to a progressive curve up to densification. Fig. 10 shows the stress-strain curve of the CFRP foldcore with UD cell wall material. In addition to quasi-static testing, dynamic compression tests at 300 s^{-1} and 500 s^{-1} were conducted on a drop tower. However, no strain rate effect occurred, i.e. the stress level was not influenced by the loading rate. The shear testing turned out to be limited by the high strength of the CFRP structure leading to a debonding between core and loading plates at some point of the experiment.

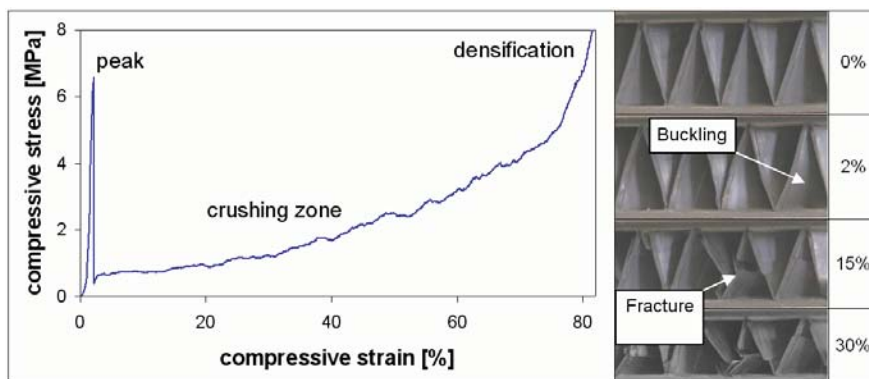


Figure 10:
 Compressive stress-strain diagram and cell wall behavior of CFRP core.

6.2 Test results for Stuttgart-type foldcores

6.2.1 Compression tests

A foldcore under flatwise compression fails with an observable buckling and folding pattern. The experimental results for flatwise compression test are reproducible, despite the complex failure mode. Corresponding test images and the stress-strain curve are shown in Fig. 11a and Fig. 11b. After an initial elastic

deformation the cell walls start to buckle and the folding edges start kinking, which is accompanied by a large drop in the stress level. For larger deformations the stress increases again, which is due to crushing behavior with paper-to-paper contacts, up to the final densification regime. This is characterised by a steep slope in the diagram.

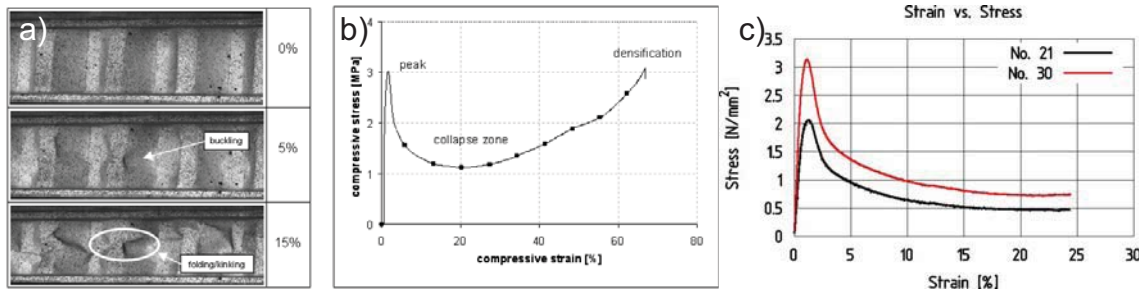


Figure 11: Pictures of foldcore sample type 31 at 0%, 5% and 15% strain (a) and stress-strain curve of foldcore type 31 (b). Stress-strain curves of foldcores type 21 and 30 (c).

Fig. 11c shows the stress-strain curves of the foldcores type 21 and 30. The peak stresses for those foldcores were 1.9 N/mm² for type 21 and 3.1 N/mm² for type 30.

6.2.2 Transverse shear tests

Six samples for each direction and each core geometry were tested during the shear test program. All the samples displayed similar overall behavior during the tests (Fig. 12). The stress applied to the core grew with increasing strain during the first part of the tests. The growth is nonlinear due to a nearly linear decrease of shear modulus with increasing shear strain. After reaching the maximum stress the bearable load dropped rapidly with increasing shear strain to a certain stress level and remained stable for a significant shear strain range. During the test where shear is applied in L-direction of the core the collapse started with buckling of the individual walls. Later ruptures parallel to the face sheets appeared. In case of type 32 foldcores, where core walls are partly cured together, the delamination of these bondings occurred in the whole sample virtually simultaneous causing an instant drop in bearable shear load. In W-direction the samples collapsed due to buckling and rupture along the folding edges of the core. The maximal stress levels are summarized in Tab. 1.

Table 1: Maximal shear stresses (aramid paper foldcores)

L-direction	Maximal shear stress	W-direction	Maximal shear stress
No. 21	1.08-1.23 N/mm ²	No. 21	0.94-1.17 N/mm ²
No. 30	1.92-2.11 N/mm ²	No. 30	1.41-1.71 N/mm ²
No. 32	3.30-4.60 N/mm ²	No. 32	2.15-2.60 N/mm ²

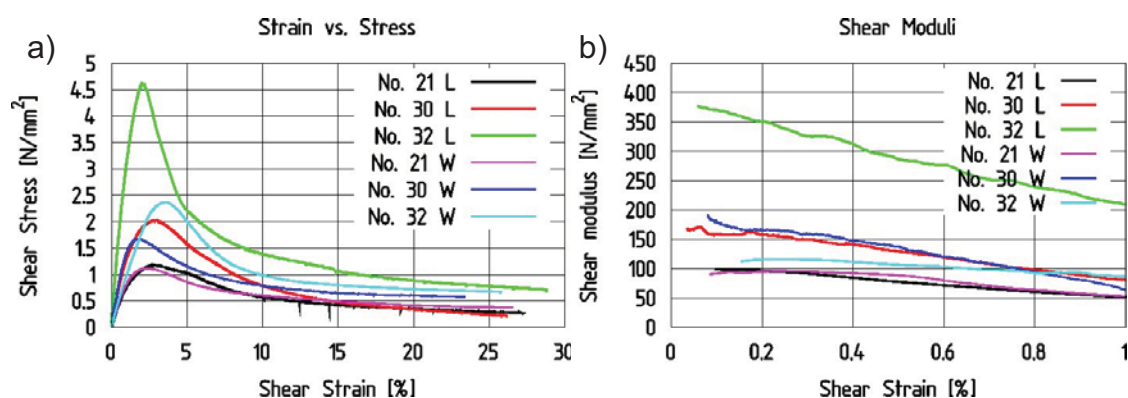


Figure 12:
Shear stress-strain diagrams (a) and shear moduli diagrams (b) for foldcores type 21, 30 and 32.

7. CONCLUSION

Foldcores from different base materials and with different unit cell geometries were produced at the Kazan State Technical University in Russia and at the University of Stuttgart in Germany.

Flatwise compression tests were performed on these foldcore sandwich structures in order to characterize their mechanical properties, show the influences of the base materials and the influences of the unit cell geometry.

Also the base material was investigated experimental; the mechanical properties were derived from tension tests, compression tests, bending tests and buckling tests.

This data is also used to support virtual testing; material data for input in the models and test data for validating the models is delivered.

REFERENCES

- [1] Khaliulin V.I., Batrakov V.V., Menyashkin D.G.: On structural and manufacturing capabilities of folded structures for use in sandwich panels, SAMPE Europe International Conference, Paris, 2007, pp. 141-148.
- [2] Zakirov I.M. and Alexeev K.A.: New folded structures for sandwich panels, SAMPE 2006, Long Beach, CA, 2006.
- [3] Kehrle R. and Drechsler K.: Manufacturing of folded core structures for technical applications, SAMPE Europe 25th International Conference, Paris, 2004, pp. 508-513.
- [4] Fischer S. and Drechsler K.: Aluminum foldcores for sandwich structure application, CELLMET2008, Cellular Metals for Structural and Functional Applications, 2nd International Symposium, Dresden, 2008.
- [5] Fischer S., Drechsler K., Kilchert S. and Johnson A.F.: Mechanical tests for Foldcore base material properties, CompTest 2008
- [6] Heimbs S., Middendorf P., Kilchert S., Johnson A.F and Maier M.: Experimental and numerical analysis of composite folded sandwich core structures in compression, Appl Compos Mater, 14(5-6), 2007, pp. 363-377.
- [7] Zenkert D.: The Handbook of Sandwich Construction, EMAS publishing, 1997